# Magnetic moment of thin film superconductors: When thickness matters

Corentin Pfaff, T. Courtois, M R Koblischka, S. Andrieu, J.-X. Lin, M. Hehn, Stéphane Mangin, K. Dumesnil, T. Hauet

# Magnetic moment of thin film superconductors: when thickness matters

C. Pfaff[1], T. Courtois[1], M. R. Koblischka[2], S. Andrieu[1],
J.-X. Lin[1], M. Hehn[1], S. Mangin[1], K. Dumesnil[1], T. Hauet[1]

1. Université de Lorraine, CNRS, IJL, F-54000, France
2. Saarland University, D-66041 Saarbrücken, Germany

The evolution of magnetic moment as a function of the applied magnetic field for a superconducting material is usually described by the so-called Bean model. We show here that this model fails to explain the magnetic response of conventional type-II superconductor films to a field applied perpendicular to the film plane, when their thickness is below 100 nm. More precisely, after zero-field cooling below the critical temperature, a positive moment forms in ascending field and an increasing negative moment develops when sweeping the field back to zero. We infer that such an inverted loop behavior in the case of low thickness films originates from a combination of low pinning, large penetration depth and large edge demagnetization field. From relaxation experiments, we demonstrate that the magnetic states along the inverted moment versus field loop are stable equilibrium states. Our findings provide some hints to further understand the High-Field Paramagnetic Meissner Effect (HFPME) reported in thin films and prove that field-cooling is not required to produce a paramagnetic-like response.

## I. INTRODUCTION

Isothermal diamagnetic response to an external magnetic field ($H$), due to Meissner currents, is a macroscopic signature of superconductivity. Below their critical temperature ($T_c$) and above their first critical field ($H_{c1}$), type-II superconductors host vortices (i.e., normal regions allowing the penetration of a magnetic flux quantum $\Phi_0 = h/2e$), which reduces the Meissner diamagnetic signal until full cancellation at the second critical field ($H_{c2}$), where the superconductor turns to normal state. Therefore, the macroscopic magnetic moment ($M$) of a superconductor is a good probe of the mixed-state of type-II superconductor and vortex lattice phases [1,2]. In contrast to this typical diamagnetic response, a paramagnetic response, consecutive to field-cooling, from above to below $T_c$, was also reported in a wide range of superconductors [3-12]. This is commonly referred to as "Paramagnetic Meissner effect" (PME) which are of two types. Low-Field PME (LFPME) consists in the appearance of a "paramagnetic" signal whose magnitude is maximum for the smallest cooling-field magnitude in Meissner state from µT to mT range [3,4]. Most often observed in granular bulk superconductors, this phenomenon is explained by an inhomogeneous superconducting transition through an inhomogeneous cooling. A further cooling down then compresses the trapped magnetic flux in the lower-$T_c$ regions and produces a non-equilibrium net paramagnetic moment [5,6]. High-Field PME (HFPME) consists in the monotonic increase of the magnetic moment from diamagnetic to "paramagnetic" as the sample is cooled down in the mixed state under a magnetic field in the range of few mT up to few Tesla [7-10]. Contrary to LFPME, the HFPME is more intense for larger fields. For bulk samples, it was speculated that, when the temperature is reduced below $T_c$ in the presence of high magnetic fields, flux lines are inhomogeneously trapped and then creep towards pinning centers like dislocations, local variations of alloy concentration or non-superconductive grains [7, 9-12]. Similar observations have been also made for 65 nm and 95 nm thick Nb films without such inhomogeneous strong pinning centers [8], so that other parameters may also promote HFPME. The impact of the sample shape on HFPME has been confirmed by Geim *et al.* in 2.5 µm-diameter and 100 nm-thick aluminum disks [13]. They demonstrated the presence of an unstable paramagnetic moment under increasing positive magnetic field, which they explain by the nucleation and compression of metastable multi-vortex state (or a single giant vortex carrying few $\Phi_0$) combined with edge-enhanced penetrating magnetic field due to the demagnetizing field of the thin disk. A deeper understanding of the parameters that influence HFPME would require additional isothermal $M$ vs. $H$ measurements for superconducting films with thicknesses below 100 nm, which are extremely rare in the literature.

In the present contribution, we report on the study of magnetic moment of thin films of various conventional type-II superconductors ($MgB_2$, NbN, Nb and V) with thicknesses ranging from 100 nm down to 5 nm, as a function of applied magnetic field ($H$) and temperature ($T$). When $H$ is applied perpendicular to the film plane, SQUID measurements reveal an inverted $M$ vs. $H$ loop as compared to typical curves for films thicker than 100 nm or bulk samples. We systematically analyzed the influence of film thickness (t) and $T$ on the stability of the observed field-induced "paramagnetic-like" state and argue that these dependences pinpoint the role of low vortex pinning, geometry-enhanced London penetration length and thin film edge demagnetization fields. Overall, we demonstrate that HFPME features can be achieved without field-cooling procedure and that isothermal creep processes explain moment relaxation previously used in the literature to characterize HFPME.

## I. EXPERIMENTAL DETAILS

Single crystal $MgB_2$ films were deposited by Molecular Beam Epitaxy (MBE) under ultra-high vacuum on sapphire (0001) single-crystal substrates. A 5 nm thick epitaxial MgO (111) buffer layer was deposited prior to $MgB_2$ in order to allow single crystal growth of $MgB_2$ [14]. The substrate temperature was maintained at 370 °C during growth. Mg was evaporated from a Knudsen cell at a 1 Å/s deposition rate while an electron gun was used for the B evaporation at a deposition rate of 0.1 Å/s. A 10 nm thick capping layer of gold or MgO protect the $MgB_2$ layer against oxidation. We verified that the capping layer does not influence the magnetometry results (not shown here). The crystalline quality, epitaxial relationships, growth mode, chemical content and surface flatness were controlled in-situ by RHEED (reflection high energy electron diffraction) and X-ray photo-emission spectroscopy, as well as ex-situ by X-ray diffraction and transmission electron microscopy (see Fig. S1 in the supplementary materials [41]). Note that epitaxial V and epitaxial Nb thin films were also grown by MBE, as well as textured Nb and NbN films with thicknesses ranging from 5 to 30 nm, by sputtering technique on a silicon substrate with a Ta buffer (3 nm) and a Pt capping layer (2 to 3 nm). These samples aim at proving that the obtained results can be generalized to all type-II superconductors. The magnetic characterizations were performed on 4.5 × 4.5 $mm^2$ samples using a commercial Quantum Design SQUID-VSM MPMS3 and PPMS9T mounted with a VSM-head. A negative linear slope due the diamagnetism of the sapphire substrate was systematically removed from all $M$ vs $H$ loops. The critical temperatures ($T_c$) of both MBE-grown $MgB_2$ and sputtered Nb films were deduced from magnetometry data and confirmed by resistance measurements performed on a PPMS9T mounted with an electrical transport rod. $T_c$ values as a function of $MgB_2$ and Nb film thickness are presented in Fig. S2 [41]. Especially, $T_c$ of $MgB_2$ only slightly increases from 30.5 to 32.5 K for t ranging from 17 nm down to 91 nm, and decreases down to zero below 17 nm, in agreement with previous reports [15,16]. Multiple factors can explain the fact that $T_c$ for our films remains lower than the $MgB_2$ bulk one (39 K) [17]. Between 30 and 90 nm, $T_c$ still slightly increases. By extrapolating this linear increase, 39K may be reached before 400 nm. We did not investigate such a thick film because of deposition method limits. Samples are capped with Au and thus they undergo a proximity effect which reduces $T_c$ as compared to the intrinsic bulk value. Finally, evaporated and sputtered films on a substrate and capped with another layer, may carry a larger density of structural defects which can affect the electron mean free path, and so $T_c$, as compared to bulk material. Finally, evaporated and sputtered films, on a substrate and capped with another layer, may carry a larger density of structural defects which can affect the electron mean free path, and so $T_c$, as compared to bulk material. Using Ginzburg-Landau equation, we extracted from electrical transport and magnetometry measurements a typical coherence length at 0 K of 4.5 ± 0.5 nm for the MBE-grown $MgB_2$ films and 12 ± 1 nm for the sputtered Nb films, in good agreement with previous reports [18,19].

## II. RESULTS AND DISCUSSION

Fig. 1(a) shows the magnetic moment versus out-of-plane magnetic field measured by SQUID-VSM at 4 K for a 91 nm thick $MgB_2$ film ($T_c$ = 32.5 K). The field sweeping rate is 1 mT/s. The red curve represents the first magnetization curve following the zero-field cooling (ZFC) procedure from 300 K down to 4 K. As expected, M = 0 at zero field after ZFC (point A in Fig. 1(a)). When increasing $H$, the moment becomes negative and decreases linearly. This diamagnetic behavior originates from edge Meissner currents that expel $H$ from the superconducting film [1,2]. The linearity is observed until $H$ reaches the so-called penetration field ($H_p$), here about 1 mT, where positive moments are added to the pure diamagnetic signal (point B in Fig.1(a)). These additional positive moments arise from the nucleation of superconducting vortices that allow $H$ to enter type-II superconductors [2]. Further increase of $H$ leads to (i) a densification of the vortices lattice (depending on the vortex lattice stability and extrinsic features like pinning sites) and (ii) attenuation of the superconductive current due to field-induced depairing of Cooper-pairs. As a result, the negative moment magnitude decreases until it reaches zero at the so-called second critical field value ($H_{c2}$), at which the film turns fully to the normal state [2,20]. In Fig.1(a), $H_{c2}$ is not reached since its value is larger than the maximum field available in our magnetometer (point C). When the field is swept back to lower values, the vortices are partially expelled out of the sample through the edges. When $H$ reaches zero (point D in Fig. 1(a)), the positive magnetic moment originates from vortices remained pinned mainly in the center of the sample. From this state, further field cycling provides a symmetric moment versus field loop [21,22]. Figure 1(b) (respectively (c)) shows the measurement sequence for the same sample but performed at 25 K (respectively 31 K), i.e., temperatures below but close to $T_c$. Considering the measurement done at 31 K, after ZFC ($M$ = 0, point E), an increasing magnetic field applied perpendicularly to the sample film still produces firstly a diamagnetic moment due to Meissner effect. Then, when $H$ overpasses $H_p$ (point F at a field lower than 1 mT), the negative moment magnitude decreases due to vortices entering the sample. Nevertheless, instead of reaching zero moment at $H_{c2}$ as at 4 K, the moment crosses first zero value for a field referred to as $H_{pos}$ in the following, then reaches a positive maximum value at around 130 mT (point G) before decreasing down to zero at $+H_{c2}$ (point H). Subsequently, when $H$ is reduced from above $+H_{c2}$, the moment becomes negative and its magnitude monotonically rises until reaching a maximum negative moment for a zero applied field (point I). Further field cycling going to above $-H_{c2}$ provides a symmetric moment versus field loop. Figure 1(b) presents the data obtained with the same procedure at 25 K. The $M(H)$ loop is a mix between the 4 K bulk-like behavior, dominant for

small applied magnetic fields, and the 31 K inverted behavior, dominant at higher fields. Interestingly, the inverted loops only occur when the external magnetic field is applied perpendicularly to the superconductive thin film. In Fig.1(d), moment vs. in-plane field loop obtained at 31 K shows bulk-like features. Our measurements show the influence of $T$, $t$ and the orientation of the applied field on the paramagnetic phase. In the following we will analyze these three parameters in greater depth.

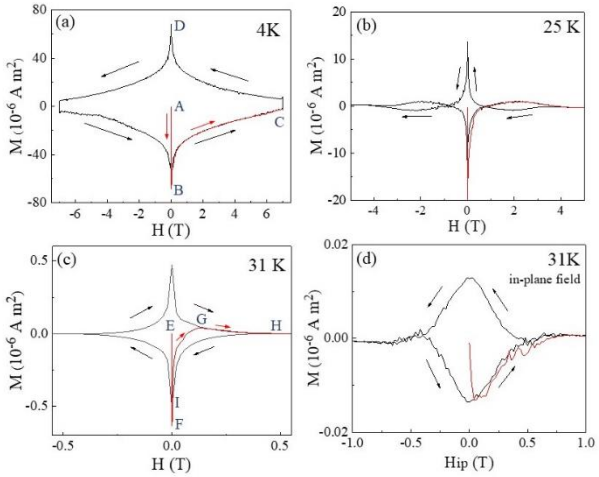


**Fig. 1. Magnetic moment (M) of a 91 nm thick $MgB_2$ film as a function of the applied magnetic field out-of-plane for (a), (b) and (c) and in-plane for (d), measured at 4 K (a), 25 K (b) and 31 K (c,d). The red line is the first magnetization curve, measured immediately after zero-field cooling from above $T_c$. The black line is the following field loop from +7 T to -7 T and back to +7 T. The external magnetic field is swept at 1 mT/s. The arrows indicate the field sweep direction. Capital letters (A-I) are used in the text for description.**

In Fig. 2, state diagrams are built for $MgB_2$ by plotting the crossing field $H_{pos}$ extracted from the first magnetization ramp and $H_{c2}$ as a function of the reduced temperature $T/T_c$ for different thicknesses. In Fig. 2(a) for $t$ = 91nm, below 0.4 $T_c$, the sample behaves as a typical bulk superconductive sample. Above 0.8 $T_c$, the *M(H)* loop is fully inverted. And in between 0.4 $T_c$ and 0.8 $T_c$, a transition from bulk-like to inverted occurs at $H_{pos}$. We can conclude that both high temperature (below $T_c$) and high field (below $H_{c2}$) favor the inverted magnetic state. The aspect ratio of the thin film being a source of discrepancy between films and bulk superconductors and between superconductive states produced by in-plane and out-of-plane external fields [23,24], we analyzed the influence of the film thickness on the inverted regime. Magnetometry measurements were performed on two $MgB_2$ films with $t$ = 45 nm ($T_c$ = 31.5 K) in Fig. 2(b) and $t$ = 15 nm ($T_c$ = 20 K) in Fig. 2(c). For $t$ =45 nm the same general trends and phase diagram as for $t$ = 91 nm are observed. However, a pure bulk-like *M(H)* loop over the full field range is no longer observed, even for temperatures as low as 0.2 $T_c$. Additionally, the fully inverted cycle exists over a broader temperature range from $T_c$ down to 0.6 $T_c$ (see zoom in inset Fig. 2(c)). These two differences are confirmed and enhanced for the $t$ = 15 nm for which only inverted loops are seen for the whole range of tested temperature. In Fig. 2(d), the full inverted loop measured at 4 K for 15 nm thick film is plotted for comparison with Fig. 1(a) for $t$ = 91 nm. At this stage, we can conclude that thin film as well as high temperatures and high magnetic fields promote inverted *M vs H* loops. Note that the observations reported here for $MgB_2$ films are confirmed for other conventional superconductor films like epitaxial V, epitaxial Nb, textured Nb, textured NbN (see Fig. S6 [41]). Figure S3 shows the case of sputtered Nb thin films with thicknesses ranging from 5 to 30 nm [41]. Besides we verified that the results do not depend on some specific field gradients inside the SQUID magnetometers [6], as demonstrated in Fig. S4 [41].

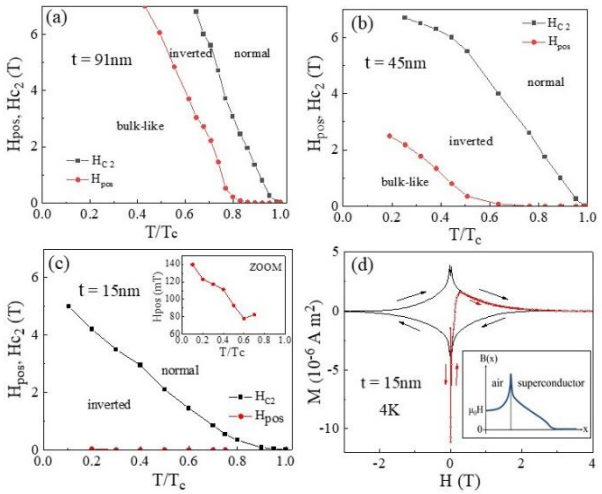


**Fig. 2. Critical field $H_{c2}$ (black squares) and transition field $H_{pos}$ (red circles) between negative and positive moment, extracted from the first field ramp after zero-field cooling, as a function of reduced temperature $T/T_c$ for $MgB_2$ films with thickness $t$ = 91 nm (a), $t$ = 45 nm (b) and $t$ =15 nm (c). These phase diagrams highlight regions where the films have negative moment (bulk like) and positive moment (inverted). $MgB_2$ is no longer superconducting in the normal region. The inset in (c) shows a zoom on linear temperature dependence of $H_{pos}$; (d) magnetic moment of a 15 nm thick $MgB_2$ film as a function of out-of-plane magnetic field, measured at $T$ = 4 K. The red line is the first magnetization curve, measured immediately after zero-field cooling from above $T_c$. Inset of (d) is a scheme of the profile of perpendicular induction $B$ as a function of position $x$ near the edge of a thin film superconductor undergoing an increasing magnetic field $H$ applied perpendicularly to the film, as presented in Ref. [26] for instance.**

The stability of the "paramagnetic-like" state, induced during the first field ramp, is further tested by moment relaxation measurements in a fixed magnetic field for $t$ = 15 nm. As shown in Fig. 3(a), after ZFC, under a constant field of 100 mT, the moment relaxes exponentially with a characteristic time ($\tau$) of 540 s towards a positive moment state while a constant field of 40 mT provides slower relaxation time $\tau$ = 890 s and smaller relaxation amplitude (see fits in Fig. S5 [41]). Therefore, we can conclude that the processes involved during the first magnetization ramp is activated by $H$. We

performed similar after-effect experiments from $H > H_{c2}$ down to negative field. In Fig. 3(b), for a low sweeping rate of 1 mT/s, as $H$ decreases from above $H_{c2}$, a negative moment rises and reaches its maximum near zero field. Modifying the field sweep rate up to 15 mT/s leads to a smaller negative, or even positive, moment (red curve in Fig. 3(b)). When stopping the field sweep at a selected value kept fixed afterwards (at about 0 mT, 100 mT and 250 mT), M relaxes from the red curve down to the main hysteresis loop (black curve in Fig. 3(b)). This relaxation is exponential and the single relaxation time (τ) decreases, i.e., the relaxation is eased, when raising temperature and/or fixed field intensity and/or when reducing the film thickness (inset in Fig. 3(b)). Overall, these relaxation experiments demonstrate that the inverted state (including the positive moment state or "paramagnetic-like" state in ascending field) is a stable equilibrium state.

Let us now consider how the film thickness can impact the magnetic response of superconductor thin film and lead to a positive moment in ascending field, at the opposite of the usual bulk superconductors diamagnetism. As theoretically studied in details in Ref. [25] and [26], the large demagnetization factor of thin film produces an enhanced value of the magnetic field in the penetrated region at the sample edge (see inset of Fig. 2(d)). Its maximum can reach $H_{edge} = H\sqrt{L/t}$ (with $L$ the typical lateral dimension of the film). In other words, a 15 nm thick superconductor film with millimetric lateral dimensions experiences, in part of the penetrated region near the edges, a field up to several hundred times larger than $H$. One direct consequence is that the field required to transit from the Meissner state to the vortex state, i.e., the field required to nucleate the first vortices, is drastically reduced in a thin film as compared to the intrinsic critical field $H_{c1}$. Indeed, the penetration field $H_p$ for a 15 nm thick $MgB_2$ film at 4 K (Fig. 2(d)) is lower than 0.5 mT, whereas $H_{c1}(0) = 110$ mT has been carefully quantified in similar single crystalline $MgB_2$ films with several microns thickness [27,28]. As already pointed out by Geim *et al.* [13], a second consequence of enhanced magnetic field at the edge is an additional paramagnetic signal to the magnetic moment of the superconductor film. Indeed, the SQUID magnetometer collects the whole magnetic flux located in the sample apart from the homogeneous external field $H$. A region of the sample where the magnetic field is larger than $H$ translates into a positive moment, as well as a region from which the field is expulsed by Meisner screening results in a negative moment. The edge region providing the additional positive magnetic moment in ascending $H$ depends on the field penetration length [26]. In thin film superconductor with thickness smaller than the bulk London penetration length $\lambda$, the effective penetration length is no longer $\lambda$ but $\Lambda = 2\lambda^2/t$ [29-32]. In a 15 nm thick film, and considering the intrinsic bulk $\lambda(0\text{ K}) \approx 100$ nm for $MgB_2$ [27,33-35], $\Lambda(0\text{ K})$ overpasses 1 µm. Since both $H_{edge}$ and $\Lambda(0\text{ K})$ increase when the film thickness shrinks, it is expected that the additional positive moment provided by the edge field rises when $t$ is reduced. The fact that $\Lambda$ increases with the sample temperature according to $\Lambda(T) = \Lambda(0)[1-(T/T_c)^4]^{-1}$ [35] is also consistent with the experimental observation that temperature favors the positive moment in ascending field after ZFC, as well as the overall inverted loop (see Fig. 1).

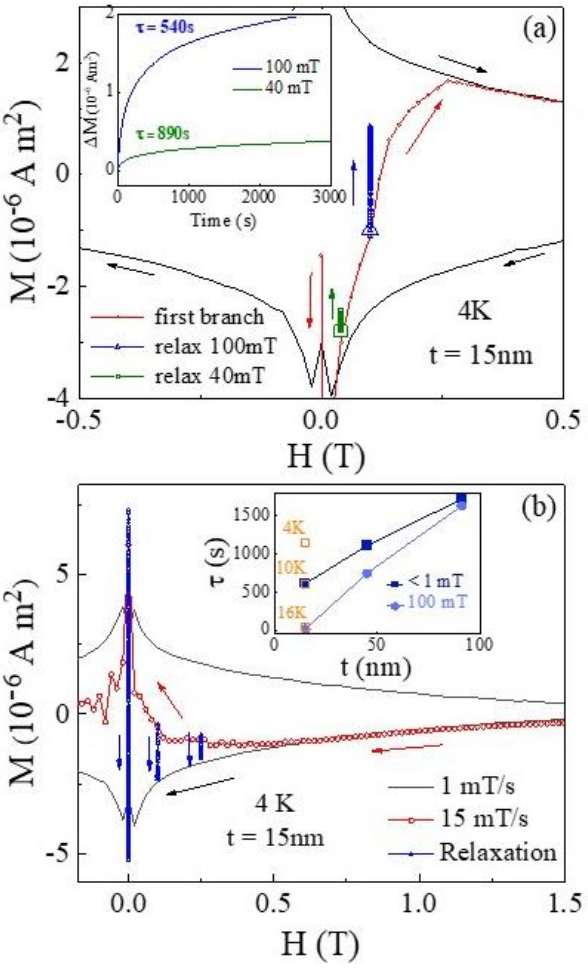


**Figure 3. (a) Full hysteresis loop (black line) and first magnetization curve (red line) measured at 4 K on a $MgB_2$ (15 nm) film. The blue triangles and the green squares are the measurements of moment versus time under a fixed field of 100 mT and 40 mT, respectively, after ZFC. In the inset to (a), the same relaxation data are plotted as a function of time. An exponential relaxation is found with relaxation time τ of 540 s for 100 mT and 890 s for 40 mT. (b) Full hysteresis loop measured at 4 K with a field sweep rate of 1 mT/s (black line) compared to the decreasing field branch from positive field above $+H_{c2}$ to negative field measured with a field sweep rate of 15 mT/s (red open circles). The blue dots correspond to the moment relaxation in constant field from three points of the red curve, respectively 250 mT, 100 mT or near zero field. The moment decrease (see blue arrows) can be fitted by an exponential function with a relaxation characteristic time ($\tau$). In inset to (b), $\tau$ values are plotted as a function of film thicknesses, for the same reduced $T/T_c = 0.5$, and for two constant fields, namely 100 mT (light blue disks) and lower than 1 mT (dark blue filled squares). Three open squares are added to show the acceleration of the relaxation when the temperature rises from 4 K to 16 K, for the 15 nm thick sample near zero field.**

At that stage, it must be noted that in real millimetric samples, scratches on the thin film, pre-existing at the substrate surface or due to sample handling, often exist and could also be source of additional effective edges. In order to further characterize the influence of the edge field effects on promoting positive magnetic moment, we performed cuts on a 45 nm thick $MgB_2$ film with a diamond saw to successively isolate 4, 8 and finally 12 regions, within the same initial sample area. By doing so, we increased the total edge length relative to the sample surface. As shown in Fig. S7(a-d), for the full film and then after each cutting step, we measured magnetization versus out-of-plane field, at 16K after zero field cooling, similar to the data presented in Fig. 1(b). As shown in Fig. S7(e), $H_{pos}$, decreases when increasing the number of cuts [41]. This means that the cutting process favors the "inverted state". It is consistent with a positive moment produced by the sample edges, although one cannot exclude that it also partially relates to a modification of the vortex nucleation at the new rough artificial edges. Nevertheless, the overall shape of the M(H) loop did not change drastically with the number of cuts. If the enhanced edge field was the leading mechanism promoting the inverted M(H) loop, one would expect to have a much more significant evolution towards a full inverted loop. It is not the case.

The contribution of edge-enhanced field to the positive moment is not enough to obtain a positive moment in the Meissner state since the volume diamagnetic moment is much larger. Nevertheless, the field-induced introduction of vortices, above $H_p$, lowers the volume diamagnetic signal and eventually allows a positive moment, for a field larger than $H_{pos}$. As shown in Fig. S8 [41], the moment variation around $H_{pos}$ is quite "reversible" as long as it does not visit a significant portion of the main hysteresis loop. Moreover, our relaxation experiments in Fig. 3 confirm that the vortex propagation is a field-activated and thermally-activated process. $H_{pos}$ decreases linearly with temperature. Vortex mobility is also affected by the film thickness since a larger density of defects is expected in thicker films, and so $H_{pos}$ rises with the film thickness. The large vortex mobility, gained in increasing the field, increasing the temperature and lowering the film thickness, must produce a decrease of the critical current $J_c$ [3, 36-38]. Therefore, one can expect a consequent decrease of the diamagnetic signal magnitude while preserving a significant positive moment signal from the vortices. This, coupled to the positive moment from the enhanced edge field, may lead to an overall positive moment.

The decrease of moment at high field up to $H_{c2}$, common to both the first magnetization curve after ZFC and the full hysteresis loop (see for instance Fig. 2(d)), can be explained by two complementary effects: i) the increasing external field allows vortices to penetrate the whole sample area and densifies the vortex lattice, thus the enhancement of the edge-field is continuously reduced since the difference between the field inside and outside the sample is gradually suppressed, ii) the Cooper pair density, and so the critical current, in the superconducting regions of the sample continuously decrease when the external field increases up to $H_{c2}$ due to orbital effect [20,39]. For a 15 nm thick film, decreasing $H$ from $H_{c2}$ leads to a negative moment whose magnitude reaches a maximum at zero field (Fig. 2(d)). Such behavior has already been observed in superconductors when the vortices are expulsed in a reversible manner in absence of strong volume pinning centers [40]. Usually, as observed in Figs. 2(a) and 2(b) for our thickest film, below a certain field, the pinning is strong enough to conserve pinned vortices in the center of the sample and to generate a remanent positive moment as in any bulk type-II superconductor. It is no longer the case for the thinnest film (Fig. 2(d)) since a reduced film thickness gives rise to a lower density of defects, as well as a stronger vortex-vortex repulsion due to the enhanced vortex extension $2\Lambda(T)$ [29]. Note that, in the descending branch from $H_{c2}$, an additional negative moment must be provided by the edge-field since the positive field magnitude inside the superconductive sample remain larger than the external field $H$.

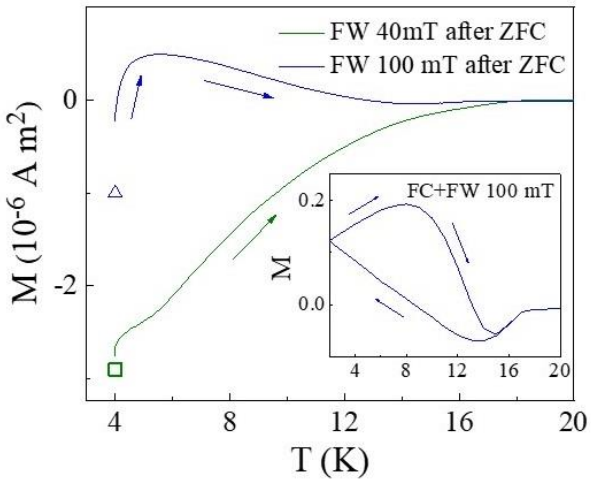


**Figure 4. Magnetic moment ($M$) as a function of temperature (T) measured on a $MgB_2$ (15nm) film during warming under fixed field (FW) of 100 mT (blue line) and 40 mT (green line), after ZFC. The two symbols indicate the same two starting points as in the relaxation experiments plotted in Fig. 3(a). The inset shows the moment measured during field cooling (FC) at 100 mT from 25 K down to 2 K, and then field warming (FW) in 100 mT from 2 K to 25 K.**

Finally, it is interesting to compare the isothermal relaxation process that we obtained as function of time in a fixed applied field in Fig. 3(a) with the one reported as a function of temperature in the case of HFPME in the literature [8,9]. In Fig. 4, after ZFC down to 4 K, $H$ was raised up to either 40 mT or 100 mT. Then under fixed field, the moment is measured during a temperature cycle from 4 K up to 24 K (i.e., above $T_c$). The single green open square and single blue open triangle correspond to ones in Fig. 3(a), at 40 mT and 100 mT respectively, before relaxation. In Fig. 4, when the temperature rises, an increase of the moment up to positive value is observed, followed by a shallower decrease, consistently with previous data obtained for Nb films [8]. This first increase

of moment is similar to the isothermal relaxation described in inset of Fig. 3(a) under 100mT. As a matter of fact, the time required to perform the $M(T)$ measurement from 4 K to 20 K is typically of the order of 1000 s. Note that similar relaxation features are seen both for $M(T)$ measurements performed after ZFC or FC in 100 mT (inset to Fig. 4) accordingly to Ref. [8]. Using a 40 mT fixed field after ZFC, instead of 100 mT, one only allows the vortex state to slightly relax and a significant negative moment remains. So, we conclude that, in thin enough films, the increase of moment during $M(T)$ leading to the so-called HFPME in Ref. [8] has the same origin as the one observed here during *M(H)* after ZFC (Fig. 3) and, therefore, that the such HFPME feature does not necessarily require a field-cooling procedure.

## IV. SUMMARY

In conclusion, we studied the $M$ vs $H$ loops of various conventional type-II superconductor films with thicknesses ranging from 100 nm down to 5 nm. The out-of-plane field hysteresis loops for the thinnest films are inverted compared to the one usually observed for bulk superconductor and described by Bean's model. In particular, after ZFC, the magnetic moment reaches a positive value when increasing the field. When decreasing the external field from above $H_{c2}$ down to zero, the moment is negative and its magnitude increases with decreasing field, leading to a negative moment at remanence. From relaxation experiments, we demonstrate that the mixed states adopted along the inverted loop are stable equilibrium states, contrary to previous reports on micron-wide disks [13]. We correlated the field, temperature and thickness dependence of these inverted loops to the large penetration length, the vortex mobility and the edge demagnetization fields which are specific features of thin films. Finally, our observations show that High-Field Paramagnetic Meissner effect (HFPME) [8] can be achieved during isothermal field sweep or by vortex relaxation under fixed field in absence of any field-cooling procedure.

## ACKNOWLEDGEMENTS

The authors thank B. Leridon, A. Silhanek and N. Lejeune for fruitful discussions. The authors thank the CC-3M at Institut Jean Lamour for the transmission electron microscopy images of $MgB_2$ films, especially S. Migot, J. Ghanbaja and M. Emo. The work was supported by the « SONOMA» project co-funded by FEDER-FSE Lorraine et Massif des Vosges 2014-2020, a European Union Program, and by the French National Research Agency through the France 2030 government grants PEPR SPIN ANR-22-EXSP 0008.

## References

[1] C. P. Poole, Jr., H. A. Farach, and R. J. Creswick, "Superconductivity", Academic Press, New York (1995).
[2] Ph. Mangin, R. Kahn. "Superconductivity: An introduction", Springer International Publishing AG (2017).
[3] M.R. Koblischka, L. Pust, C.S. Chang, T. Hauet, A. Koblischka-Veneva, The Paramagnetic Meissner Effect (PME) in Metallic Superconductors, Metals 13, 1140 (2023).
[4] M.S. Li, Paramagnetic Meissner effect and related dynamical phenomena, Phys. Rep. 376 133 (2003).
[5] A. E. Koshelev and A. I. Larkin, Paramagnetic moment in field-cooled superconducting plates: Paramagnetic Meissner effect, Phys. Rev. B 52, 13559 (1995).
[6] P. Kostic, B. Veal, A. P. Paulikas, U. Welp, V. R. Todt, C. Gu, U. Geiser, J. M. Williams, K. D. Carlson, R. A. Klemm, Paramagnetic Meissner effect in Nb, Phys. Rev. B 53, 791 (1996).
[7] A. I. Rykov, S. Tajima, and F. V. Kusmartsev, High-field paramagnetic effect in large crystals of $YBa_2Cu_3O_{7-\delta}$, Phys. Rev. B 55, 8557 (1997).
[8] A. Terentiev, D. B. Watkins, L. E. De Long, D. J. Morgan, and J. B. Ketterson, Paramagnetic relaxation and Wohlleben effect in field-cooled Nb thin films, Phys. Rev. B 60, R761 (1999).
[9] F.T. Dias, P. Pureur, P. Jr. Rodrigues, and X. Obradors, Paramagnetic effect at low and high magnetic fields in melt-textured $YBa_2Cu_3O_{7-\delta}$, Phys. Rev. B 70, 224519 (2004).
[10] S.K. Ramjan, L.S. Sharath Chandra, Rashmi Singh and M. K. Chattopadhyay, Strong paramagnetic response in the superconducting state of Y-containing $V_{0.6}Ti_{0.4}$ alloys, Supercond. Sci. Technol. 35, 105006 (2022).
[11] Shyam Sundar, M.K. Chattopadhyay, L.S. Sharath Chandra and S.B. Roy, High field paramagnetic Meissner effect in $Mo_{100-x}Re_x$ alloy superconductors, Supercond. Sci. Technol. 28, 075011 (2015).
[12] M. Matin, M. K. Chattopadhyay, L. S. Sharath Chandra and S. B. Roy, High-field paramagnetic Meissner effect and flux creep in low-Tc Ti–V alloy superconductors, Supercond. Sci. Technol. 29, 025003 (2016).
[13] A. K. Geim, S. V. Dubonos, J. G. S. Lok, M. Henini, and J. C. Maan, Paramagnetic Meissner effect in small superconductors, Nature (London) 396, 144 (1998).
[14] L. Li, H. Zhang, Y.-H. Yang and G.-X. Miao, High-Quality Epitaxial $MgB_2$ Josephson Junctions Grown by Molecular Beam Epitaxy, Adv. Engineer. Mater. 19, 1600792 (2017).
[15] C. Zhang, Y. Wang, D. Wang, Y. Zhang, Z.-H. Liu, Q.-R. Feng, Z.-Z. Gan, Suppression of superconductivity in epitaxial MgB2 ultrathin films, J. Appl. Phys. 114, 023903 (2013).
[16] M. Naito and K. Ueda, $MgB_2$ thin films for superconducting electronics, Supercond. Sci. Technol. 17, R1 (2004).
[17] W. N. Kang, Hyeong-Jin Kim, Eun-Mi Choi, C. U. Jung, Sung-Ik Lee, $MgB_2$ superconducting thin films with a transition temperature of 39 kelvin, Science 292, 1521 (2001).
[18] S Patnaik, L D Cooley, A Gurevich, A A Polyanskii, J Jiang, X Y Cai, A A Squitieri, M T Naus, M K Lee, J H Choi, Electronic anisotropy, magnetic field-temperature phase diagram and their dependence on resistivity in c-axis oriented $MgB_2$ thin films, Supercond. Sci. Technol. 14, 315 (2001).
[19] P. Quarterman, N. Satchell, B.J. Kirby, R. Loloee, G. Burnell, N.O. Birge, J. A. Borchers, Distortions to the penetration depth and coherence length of superconductor/normal-metal superlattices, Phys. Rev. Mater 4, 074801 (2020).
[20] D. V. Shantsev, Y. M. Galperin, T. H. Johansen, Thin superconducting disk with field-dependent critical current: Magnetization and ac susceptibilities, Phys. Rev. B 61, 9699 (2000).

[21] C. P. Bean, Magnetization of Hard Superconductors, Phys. Rev. Lett., 250 (1962).
[22] D.-X. Chen and R. B. Goldfarb, Kim model for magnetization of type-II superconductors, J. Appl. Phys. 66, 2489 (1989).
[23] F.E. Harper and M. Tinkham, The Mixed State in Superconducting Thin Films, Phys. Rev. 172, 441 (1968).
[24] M. Tinkham, Introduction to Superconductivity, McGraw-Hill, New York (1996).
[25] E. Zeldov, J.R. Clem, M. McElfresh, M. Darwin, Magnetization and transport currents in thin superconducting films, Phys. Rev. B 49, 9802 (1994).
[26] E.H. Brandt, Theory of type-II superconductors with finite London penetration depth, Phys. Rev. B 64, 024505 (2001).
[27] L. Lyard, T. Klein, J. Marcus, R. Brusetti, C. Marcenat, M. Konczykowski, V. Mosser, K. H. Kim, B. W. Kang, H. S. Lee, and S. I. Lee, Geometrical barriers and lower critical field in $MgB_2$ single crystals, Phys. Rev. B 70, 180504(R) (2004).
[28] B. Kang, H.-J. Kim, M.-S. Park, K.-H. Kim, and S.-I. Lee, Reversible magnetization of MgB2 single crystals with a two-gap nature, Phys. Rev. B 69, 144514 (2004).
[29] J. Pearl, Current distribution in superconducting films carrying quantized fluxoids, Appl. Phys. Lett. 5, 65 (1964).
[30] J. R. Clem, Two-dimensional vortices in a stack of thin superconducting films: A model for high-temperature superconducting multilayers, Phys. Rev. B 43, 7837 (1991).
[31] L. Embon, Y. Anahory, Ž.L. Jelić, E.O. Lachman, Y. Myasoedov, M.E. Huber, G.P. Mikitik, A.V. Silhanek, M.V. Milošević, A. Gurevich, E. Zeldov, Imaging of super-fast dynamics and flow instabilities of superconducting vortices, Nature Commun. 8, 85 (2017).
[32] L. Ceccarelli, D. Vasyukov, M. Wyss, G. Romagnoli, N. Rossi, L. Moser, and M. Poggio, Imaging pinning and expulsion of individual superconducting vortices in amorphous MoSi thin films, Phys. Rev. B 100, 104504 (2019).
[33] C. Buzea and T. Yamashita, Review of superconducting properties of $MgB_2$, Supercond. Sci. Technol. 14 R115 (2001).
[34] D.K. Finnemore, J.E. Osbenson, S.L. Budko, G. Lapertot, P.C. Canfield, Thermodynamic and Transport Properties of Superconducting $Mg^{10}B_2$ Phys. Rev. Lett. 86, 2420 (2001).
[35] T. Nishio, S. Okayasu, J. Suzuki, N. Kokubo, and Kazuo Kadowaki, Observation of an extended magnetic field penetration in amorphous superconducting MoGe films, Phys. Rev. B 77, 052503 (2008).
[36] C.J. van der Beek, M. Konczykowski, A. Abal'oshev, I. Abal'osheva, P. Gierlowski, S.J. Lewandowski, M.V. Indenbom, S. Barbanera, Strong pinning in high-temperature superconducting films, Phys. Rev. B 66, 024523 (2002).
[37] T. Shapoval, H. Stopfel, S. Haindl, J. Engelmann, D. S. Inosov, B. Holzapfel, V. Neu, and L. Schultz, Quantitative assessment of pinning forces and magnetic penetration depth in NbN thin films from complementary magnetic force microscopy and transport measurements, Phys. Rev. B 83, 214517 (2011).
[38] C.J. van Der Beek, chapter "Flux Pinning" in Handbook of superconductivityDavid editors D.A. Cardwell, D.C. Larbalestier, A. Braginski, Edition, 2, CRC Press (2022).
[39] E.H. Brandt, Superconductor disks and cylinders in an axial magnetic field. I. Flux penetration and magnetization curves, Phys. Rev. B 58, 6506 (1998).
[40] J.D. Livingston, Magnetic Properties of Superconducting Lead-Base Alloys, Phys. Rev. 129, 1943 (1963).
[41] See Supplemental Material at [URL will be inserted by publisher].